

Fig. 6. MeV-HL-induced shut-off in eIF2 α WT and S51A expressing cells. (a) eIF2 α was detected by Western blotting assay using antibodies against phospho-eIF2 α (upper panel), or eIF2 α (lower panel) on the same membrane. The ratio of phosphorylated eIF2 α (vs. mock infected B95a-2 α WT) is shown under each lane. (b) Protein synthesis in MeV-HL-infected B95a-2 α WT (wt) and B95a-2 α S51A (S) cells was examined similar to Fig. 1a. Viral proteins are indicated to the right of the image. (c) The rates of host protein synthesis in B95a-2 α WT cells (closed circle) or B95a-2 α S51A (closed square) were determined from Fig. 6b by quantitation similar to Fig. 1b.

and independent of cell type. Similarly to MeV, Smith et al. reported that ability of reovirus to induce the shut-off of host protein synthesis is dependent of the viral strain [28].

The shut-off of host protein synthesis by virus infection was reported to be caused by a number of mechanisms such as inhibition of transcription, degradation of host mRNA and inhibition of translation. As the level of GAPDH mRNA was unaltered in MeV-HL-infected B95a cells, the shut-off by MeV-HL is suggested to be caused by inhibition of translation.

The shut-off of host translation is caused mainly by inhibition of the cap-dependent mechanism [6]. Contrary to many other virus-infected cells in which the components of the eIF4F complex including eIF4G, eIF4E and 4E-BP1 are involved in cap-dependent translation, they were not modified by MeV-HL infection. Therefore, the cap-binding activity of eIF4F complex appears to be intact. Instead, phosphorylation of eIF2 α in MeV-HL-infected B95a cells was noted (Fig. 5). The phosphorylation rate of eIF2 α correlated with the inhibition of host protein synthesis after MV infection. In addition, in B95a-2 α S51A cells that stably expressed the eIF2 α -S51A mutant, the shut-off phenomenon appeared to be suppressed compared with those in B95a and B95a-2 α WT cells (Fig. 6). Therefore, phosphorylation of eIF2 α is suggested as one of the mechanisms particularly at the early stage for the induction of host shut-off by MeV-HL infection.

Conner and Lyles reported that phosphorylation of eIF2 α in VSV-infected cells suppressed viral translation rather than host translation [22]. In the case of MeV-HL infection, the suppression effect on host proteins was obviously much greater than that on viral proteins (Figs. 1a and 6b). MeV-HL mRNA may be more resistant to the effect of phosphorylated eIF2 α than cellular mRNA. The mechanisms of the selective synthesis of viral protein in the shutoff stage of MeV-HL-infected cells are currently under investigation.

Recently, we also reported that the N protein of MeV-HL inhibits host translation by the binding to eIF3-p40 [13]. In our report, the inhibitory effect of the N protein is partial and inhibitory rate reaches a plateau at approximately 50–60%. On the other hand, MeV-HL-infection suppressed about 90% of the host translation (Fig. 1b). Experiment using eIF2 α S51A mutant in this study, in which the inhibition of eIF2 α phosphorylation observed in 18 hpi lasted 24 hpi (data not shown) showed that the shut-off was inhibited at 18 hpi but became partial after 24 hpi (Fig. 6c). The expression level of the N protein increases rapidly after 18 hpi and reaches a peak at 24 hpi (data not shown). Taken together, we hypothesize that in MeV-HL-infected B95a cells the accumulation of phosphorylated eIF2 α probably resulting from the replication of viral genome occurs at a relatively early stage of infection initiating the shut-off and then binding of increased N protein binds to eIF3-p40 and enhance the shut-off of host translation at later stage of infection.

Acknowledgement

This work was supported by grants from the Ministry of Education, Culture, Sports, Science and Technology of Japan, and the Bio-oriented Technology Research Advance Institution.

References

- [1] Lyles DS. Cytopathogenesis and inhibition of host gene expression by RNA viruses. *Microbiol Mol Biol Rev* 2000;64(4):709–24.
- [2] Abreu SL, Lucas-Lenard J. Cellular protein synthesis shutoff by mengovirus: translation of nonviral and viral mRNA's in extracts from uninfected and infected Ehrlich ascites tumor cells. *J Virol* 1976;18(1):182–94.
- [3] Kaufmann Y, Coldstein E, Penman S. Poliovirus-induced inhibition of polypeptide initiation in vitro on native polyribosomes. *Proc Natl Acad Sci USA* 1976;73(6):1834–8.
- [4] Svitkin YV, Ginevskaya VA, Ugarova TY, Agol VI. A cell-free model of the encephalomyocarditis virus-induced inhibition of host cell protein synthesis. *Virology* 1978;87(1):199–203.
- [5] Hiremath LS, Webb NR, Rhoads RE. Immunological detection of the messenger RNA cap-binding protein. *J Biol Chem* 1985;260(13):7843–9.
- [6] Gale Jr M, Tan SL, Katze MG. Translational control of viral gene expression in eukaryotes. *Microbiol Mol Biol Rev* 2000;64(2):239–80.
- [7] Yoshikawa Y, Mizumoto K, Yamanouchi K. Characterization of messenger RNAs of measles virus. *J Gen Virol* 1986;67(Pt 12):2807–12.
- [8] Wechsler SL, Fields BN. Intracellular synthesis of measles virus-specified polypeptides. *J Virol* 1978;25(1):285–97.
- [9] Graves MC. Measles virus polypeptides in infected cells studied by immune precipitation and one-dimensional peptide mapping. *J Virol* 1981;38(1):224–30.
- [10] Kobune F, Takahashi H, Terao K, Ohkawa T, Ami Y, Suzaki Y, et al. Nonhuman primate models of measles. *Lab Anim Sci* 1996;46(3):315–20.
- [11] Kobune F, Sakata H, Sugiura A. Marmoset lymphoblastoid cells as a sensitive host for isolation of measles virus. *J Virol* 1990;64(2):700–5.
- [12] Kai C, Yamanouchi K, Sakata H, Miyashita N, Takahashi H, Kobune F. Nucleotide sequences of the M gene of prevailing wild measles viruses and a comparison with subacute sclerosing panencephalitis virus. *Virus Genes* 1996;12(1):85–7.
- [13] Sato H, Masuda M, Kanai M, Tsukiyama-Kohara K, Yoneda M, Kai C. Measles virus N protein inhibits host translation by binding to eIF3-p40. *J Virol* 2007;81(21):11569–76.
- [14] Tsukiyama-Kohara K, Poulin F, Kohara M, DeMaria CT, Cheng A, Wu Z, et al. Adipose tissue reduction in mice lacking the translational inhibitor 4E-BP1. *Nat Med* 2001;7(10):1128–32.
- [15] Devaney MA, Vakharia VN, Lloyd RE, Ehrenfeld E, Grubman MJ. Leader protein of foot-and-mouth disease virus is required for cleavage of the p220 component of the cap-binding protein complex. *J Virol* 1988;62(11):4407–9.
- [16] Etchison D, Milburn S, Ederly I, Sonenberg N, Hershey JW. Inhibition of HeLa cell protein synthesis following poliovirus infection correlates with the proteolysis of a 220,000-dalton polypeptide associated with eukaryotic initiation factor 3 and a cap binding protein complex. *J Biol Chem* 1982;257(24):14806–10.
- [17] Etchison D, Fout S. Human rhinovirus 14 infection of HeLa cells results in the proteolytic cleavage of the p220 cap-binding complex subunit and inactivates globin mRNA translation in vitro. *J Virol* 1985;54(2):634–8.
- [18] Feigenblum D, Schneider RJ. Modification of eukaryotic initiation factor 4F during infection by influenza virus. *J Virol* 1993;67(6):3027–35.
- [19] Hershey Jr WB, Mathews MB, Sonenberg N. Translational control. Plainview, NY: Cold Spring Harbor Laboratory Press; 1996.
- [20] Zhang Y, Feigenblum D, Schneider RJ. A late adenovirus factor induces eIF4E dephosphorylation and inhibition of cell protein synthesis. *J Virol* 1994;68(11):7040–50.
- [21] Mahalingam M, Cooper JA. Phosphorylation of mammalian eIF4E by Mnk1 and Mnk2: tantalizing prospects for a role in translation. *Prog Mol Subcell Biol* 2001;27:132–42.
- [22] Connor JH, Lyles DS. Inhibition of host and viral translation during vesicular stomatitis virus infection. *J Biol Chem* 2005;280(14):13512–9.
- [23] Gingras AC, Svitkin Y, Belsham GJ, Pause A, Sonenberg N. Activation of the translational suppressor 4E-BP1 following infection with encephalomyocarditis virus and poliovirus. *Proc Natl Acad Sci USA* 1996;93(11):5578–83.

- [24] Clemens MJ. Regulation of eukaryotic protein synthesis by protein kinases that phosphorylate initiation factor eIF-2. *Mol Biol Rep* 1994;19(3):201–10.
- [25] Williams BR. PKR; a sentinel kinase for cellular stress. *Oncogene* 1999;18(45):6112–20.
- [26] Treiman M, Caspersen C, Christensen SB. A tool coming of age: thapsigargin as an inhibitor of sarcoplasmic reticulum Ca^{2+} -ATPases. *Trends Pharmacol Sci* 1998;19(4):131–5.
- [27] Srivastava SP, Kumar KU, Kaufman RJ. Phosphorylation of eukaryotic translation initiation factor 2 mediates apoptosis in response to activation of the double-stranded RNA-dependent protein kinase. *J Biol Chem* 1998;273(4):2416–23.
- [28] Smith JA, Schmechel SC, Williams BR, Silverman RH, Sciff LA. Involvement of the interferon-regulated antiviral proteins PKR and RNase L in reovirus-induced shutoff of cellular translation. *J Virol* 2005;79(4):2240–50.

ATF4-Mediated Induction of 4E-BP1 Contributes to Pancreatic β Cell Survival under Endoplasmic Reticulum Stress

Suguru Yamaguchi,^{1,3} Hisamitsu Ishihara,^{1,*} Takahiro Yamada,¹ Akira Tamura,¹ Masahiro Usui,¹ Ryu Tominaga,¹ Yuichiro Munakata,¹ Chihiro Satake,¹ Hideki Katagiri,² Fumi Tashiro,⁴ Hiroyuki Aburatani,⁵ Kyoko Tsukiyama-Kohara,⁶ Jun-ichi Miyazaki,⁴ Nahum Sonenberg,⁷ and Yoshitomo Oka¹

¹Division of Molecular Metabolism and Diabetes

²Division of Advanced Therapeutics for Metabolic Diseases, Center for Translational and Advanced Animal Research
Tohoku University Graduate School of Medicine, Sendai, Miyagi 980-8575, Japan

³Institute for International Advanced Research and Education, Tohoku University, Sendai, Miyagi 980-8578, Japan

⁴Division of Stem Cell Regulation Research, Osaka University Graduate School of Medicine, Suita, Osaka 565-0871, Japan

⁵Research Center for Advanced Science and Technology, University of Tokyo, Tokyo 153-8904, Japan

⁶Department of Experimental Phylaxiology, Faculty of Medical and Pharmaceutical Sciences, Kumamoto University,
Kumamoto 860-8556, Japan

⁷Department of Biochemistry and McGill Cancer Centre, McGill University, Montreal, QC H3G 1Y6, Canada

*Correspondence: hisamitsu-ishihara@mail.tains.tohoku.ac.jp

DOI 10.1016/j.cmet.2008.01.008

SUMMARY

Endoplasmic reticulum (ER) stress-mediated apoptosis may play a crucial role in loss of pancreatic β cell mass, contributing to the development of diabetes. Here we show that induction of 4E-BP1, the suppressor of the mRNA 5' cap-binding protein eukaryotic initiation factor 4E (eIF4E), is involved in β cell survival under ER stress. 4E-BP1 expression was increased in islets under ER stress in several mouse models of diabetes. The *Eif4ebp1* gene encoding 4E-BP1 was revealed to be a direct target of the transcription factor ATF4. Deletion of the *Eif4ebp1* gene increased susceptibility to ER stress-mediated apoptosis in MIN6 β cells and mouse islets, which was accompanied by deregulated translational control. Furthermore, *Eif4ebp1* deletion accelerated β cell loss and exacerbated hyperglycemia in mouse models of diabetes. Thus, 4E-BP1 induction contributes to the maintenance of β cell homeostasis during ER stress and is a potential therapeutic target for diabetes.

INTRODUCTION

Recent studies have shown decreased pancreatic β cell mass to be a common feature of subjects with type 2 diabetes mellitus (Butler et al., 2003). Susceptibility to stress-induced apoptosis may underlie β cell loss. Translational regulation is an essential strategy by which cells cope with stress conditions (Clemens, 2001). Translation of eukaryotic mRNA is regulated primarily at the level of initiation. Translational initiation begins with formation of a ternary complex composed of the methionine-charged initiator tRNA, eukaryotic initiation factor 2 (eIF2), and GTP (Holcik

and Sonenberg, 2005). The ternary complex then binds to the 40S ribosomal subunit and several other initiation factors, generating the 43S preinitiation complex. The mRNA 5' cap-binding protein eIF4E associates with eIF4A and eIF4G to form the eIF4F complex and interacts with the 5' cap structure of the mRNA. The eIF4F complex then recruits the 43S preinitiation complex to the mRNA, allowing the complex to scan toward the initiator AUG codon. The two best characterized regulatory steps in this translational control are formation of the ternary complex and assembly of the eIF4F complex. Phosphorylation of the α subunit of eIF2 (eIF2 α) prevents ternary complex formation and thereby suppresses global translation. In addition, eIF4E-binding proteins (4E-BPs) inhibit eIF4F assembly by competitively displacing eIF4G from eIF4E. Global translational suppression through eIF2 α phosphorylation is a mechanism shared among different stress-response pathways. Depending on the nature of the stress stimulus, eIF2 α can be phosphorylated by four different kinases (Holcik and Sonenberg, 2005). Global attenuation of protein biosynthesis then paradoxically increases expression of several proteins, including the transcription factor ATF4 (Harding et al., 2000).

Because of their high insulin secretory activity, β cells are vulnerable to endoplasmic reticulum (ER) stress, a condition of disrupted ER homeostasis due to accumulation of misfolded proteins (Schroder and Kaufman, 2005). Cells respond to ER stress by activating an adaptive cellular response known as the unfolded protein response (UPR). Under ER stress conditions, global translation is suppressed through eIF2 α phosphorylation by an ER-resident kinase, PERK. The importance of PERK-mediated translational suppression has been demonstrated in infancy-onset diabetes and skeletal defects caused by loss of PERK in humans (Delepine et al., 2000) and mice (Harding et al., 2001; Zhang et al., 2002). However, the roles of translational control through inhibition of eIF4F assembly by 4E-BPs under stress conditions, including ER stress, have yet to be fully clarified. Herein, we have studied roles of 4E-BP1,

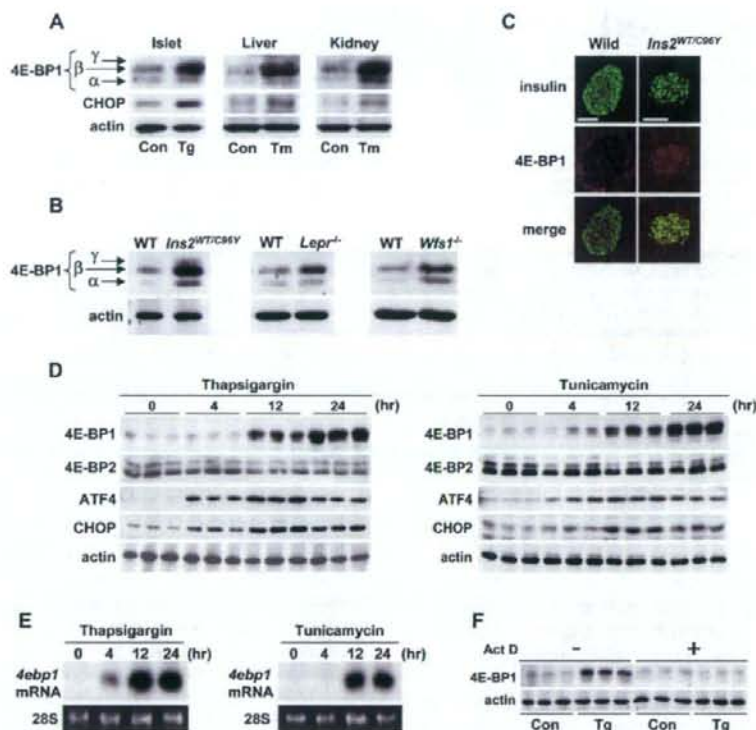


Figure 1. ER Stress Induces 4E-BP1 Expression

(A) Expression of 4E-BP1 protein in isolated islets treated with vehicle (0.05% DMSO) control (Con) or 0.5 μ M thapsigargin (Tg) for 12 hr. 4E-BP1 expression was also examined in the livers and kidneys of mice that had received intraperitoneal injections of tunicamycin (Tm) 96 hr previously.

(B) Expression of 4E-BP1 protein in islets from wild-type (WT), *Ins2*^{WT/C96Y}, *Lepr*^{-/-}, and *Wfs1*^{-/-} mice.

(C) Immunostaining of pancreatic sections from WT and *Ins2*^{WT/C96Y} mice using anti-insulin and anti-4E-BP1 antibodies. Scale bars = 50 μ m.

(D and E) Time courses of 4E-BP1, 4E-BP2, ATF4, and CHOP expression (D) and *4ebp1* mRNA expression (E) in MIN6 cells treated with thapsigargin (left panel) or tunicamycin (right).

(F) Inhibition of 4E-BP1 induction by actinomycin D (1 μ g/ml) in MIN6 cells treated with thapsigargin for 12 hr.

one of three isoforms of the 4E-BP family, in β cells under ER stress.

RESULTS

ER Stress Induces 4E-BP1

4E-BP1 protein is present in three forms with different phosphorylation states. The hypophosphorylated α and β forms are active and the hyperphosphorylated γ form is inactive in terms of eIF4E binding. Expression of 4E-BP1 protein, especially the hypophosphorylated forms, was markedly induced, with an increase in CHOP, a stress marker protein, in isolated islets treated with thapsigargin (an ER Ca^{2+} pump inhibitor causing ER stress) (Figure 1A). 4E-BP1 induction was also observed in liver and kidneys of mice administered tunicamycin (a protein glycosylation inhibitor), another ER stress inducer (Figure 1A).

Furthermore, 4E-BP1 protein expression was markedly increased in *Ins2*^{WT/C96Y} islets (Figures 1B and 1C), in which mis-

folded insulin molecules with a C96Y mutation cause ER stress (Wang et al., 1999). Islets from leptin receptor null (*Lepr*^{-/-}) mice, which have been shown to suffer from ER stress (Laybutt et al., 2007), also exhibited increased 4E-BP1 expression (Figure 1B). The *Wfs1*^{-/-} mouse (Ishihara et al., 2004) is a model of Wolfram syndrome, which is characterized by juvenile-onset diabetes mellitus and optic atrophy and is caused by *WFS1* mutations (Inoue et al., 1998; Strom et al., 1998). *WFS1*-deficient islets are affected by chronic ER stress (Ishihara et al., 2004; Riggs et al., 2005). Again, 4E-BP1 protein was increased in *Wfs1*^{-/-} islets (Figure 1B).

Induction of 4E-BP1 by ER stress was also observed in insulinoma MIN6 cells (Miyazaki et al., 1990) (Figure 1D). Expression of 4E-BP2, another member of the 4E-BP family, remained unchanged. While expression of ATF4 and CHOP peaked at 12 hr after treatment with thapsigargin or tunicamycin, 4E-BP1 protein was further increased at 24 hr posttreatment (Figure 1D). 4E-BP1 protein induction appeared to result from transcriptional

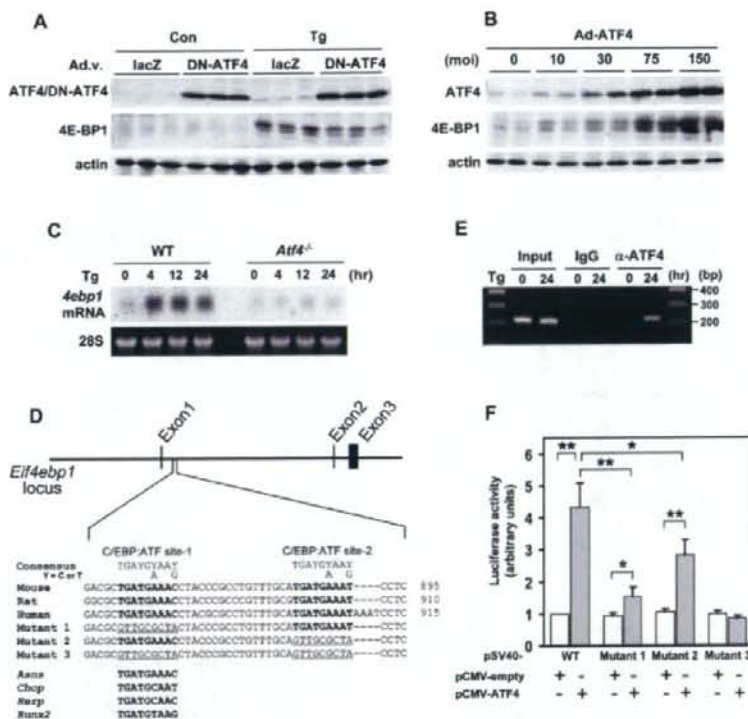


Figure 2. *Eif4ebp1* Is a Direct Target of ATF4

(A) Suppression of thapsigargin (Tg, 0.5 μ M)-induced 4E-BP1 expression by dominant-negative ATF4 (DN-ATF4). MIN6 cells were infected with an adenovirus expressing either lacZ or DN-ATF4. Two days later, the cells were treated with vehicle (0.05% DMSO) control (Con) or Tg for 12 hr. (B) 4E-BP1 expression in MIN6 cells infected with an adenovirus expressing wild-type ATF4 at the indicated multiplicity of infection (mol). (C) *4ebp1* mRNA levels in wild-type and *Atf4*^{-/-} MEFs treated with thapsigargin. (D) C/EBP-ATF composite sites in intron 1 of the *Eif4ebp1* gene. Mouse, rat, and human *Eif4ebp1* gene segments are aligned with ATF4 binding sequences in several genes. Numbers are positions relative to A of the initial ATG codon. *Asns*, asparagine synthetase; *Herp*, homocysteine-induced ER protein; *Runx2*, runt-related transcription factor 2. (E) Chromatin immunoprecipitation assay of MIN6 cells treated with thapsigargin. DNAs precipitated with nonspecific or anti-ATF4 IgG were amplified using primers for the *Eif4ebp1* intron 1 region. (F) ATF4 induction of luciferase reporters with the SV40 promoter and an *Eif4ebp1* gene segment with C/EBP-ATF composite sites or their mutants shown in (D). MIN6 cells were transfected with luciferase reporters together with either pCMV-empty or pCMV-ATF4. Error bars represent SEM. $n = 4$; * $p < 0.05$, ** $p < 0.01$.

activation since *4ebp1* mRNA levels were also increased by these ER stress inducers (Figure 1E) and the transcriptional inhibitor actinomycin D completely blocked 4E-BP1 induction by thapsigargin (Figure 1F).

ATF4 Directly Activates the *Eif4ebp1* Gene

MIN6 cells were infected with recombinant adenoviruses expressing dominant-negative (DN) forms of transcription factors involved in the UPR. Expression of DN-ATF4 (He et al., 2001) (Figure 2A), but not DN-ATF6 or DN-XBP1 (see Figure S1 available online), suppressed 4E-BP1 induction by thapsigargin. Conversely, expression of wild-type ATF4 dramatically induced 4E-BP1 expression (Figure 2B). Furthermore, *4ebp1* mRNA levels were not increased by thapsigargin in *Atf4*^{-/-}

murine embryonic fibroblasts (MEFs) (Harding et al., 2003) (Figure 2C).

A survey of the mouse *Eif4ebp1* gene using a luciferase assay identified a segment in intron 1 that conferred thapsigargin sensitivity to a luciferase reporter (Figure S2). Indeed, we found two potential ATF4 binding sequences (C/EBP:ATF composite sites) in this segment (Figure 2D). Chromatin immunoprecipitation (ChIP) assays revealed that ATF4 binds this segment (Figure 2E). Furthermore, cotransfection of a luciferase reporter containing the C/EBP:ATF sites with an ATF4-expressing plasmid increased luciferase activity by 4.3-fold (Figure 2F). Disruption of the upstream C/EBP:ATF site (mutant 1) or the downstream site (mutant 2) decreased the ATF4-mediated increase in luciferase activity by 83% or 47%, respectively, and disruption of both (mutant 3) completely abolished the increase (Figure 2F).

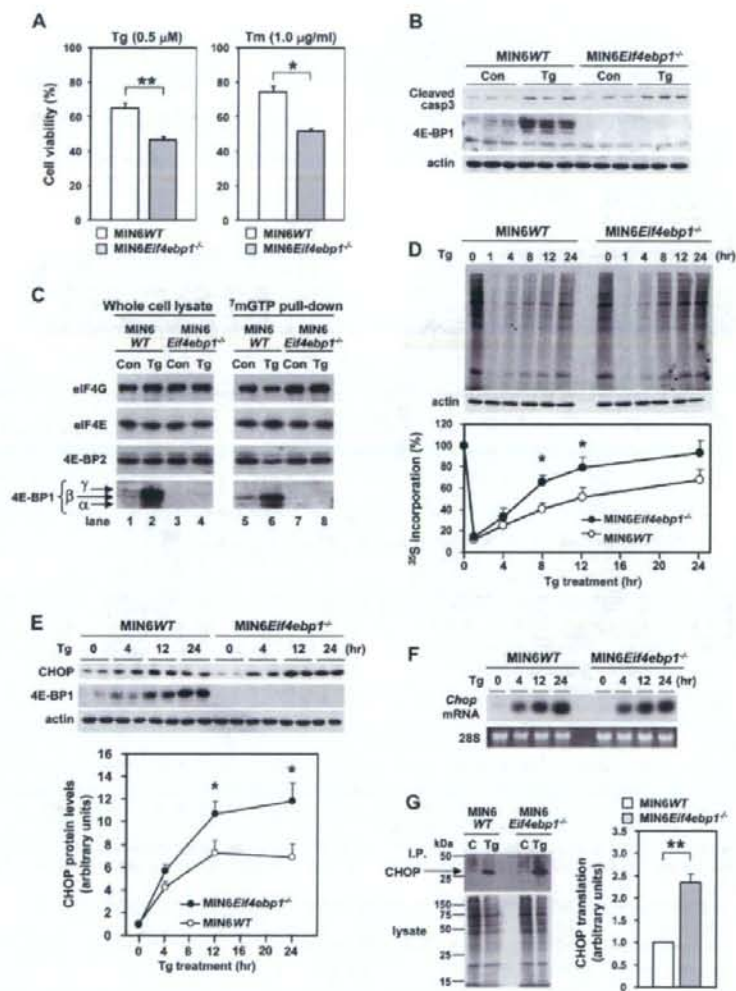


Figure 3. 4E-BP1-Deficient Cells Exhibit Increased Apoptosis Susceptibility with Deregulated Translational Control

(A) Viability of MIN6WT and MIN6Ei4ebp1^{-/-} cells treated with 0.5 μ M thapsigargin (Tg) or 1.0 μ g/ml tunicamycin (Tm) for 36 hr, normalized to MIN6WT cells treated with vehicle (0.05% DMSO). n = 3–4.

(B) Immunoblot of cleaved caspase-3 in MIN6WT and MIN6Ei4ebp1^{-/-} cells treated with vehicle control (Con) or thapsigargin for 24 hr.

(C) Immunoblot analysis of 4E-BP1, 4E-BP2, eIF4E, and eIF4G in whole-cell lysates (left) or in a complex associated with 7mGTP-Sepharose (right) in cells treated with thapsigargin for 24 hr.

(D) [³⁵S]methionine/cysteine incorporation during a 15 min pulse labeling in MIN6WT and MIN6Ei4ebp1^{-/-} cells pretreated with thapsigargin for the indicated periods. Ten percent of the lysates were also probed with an anti-actin antibody. A representative autoradiogram is shown in the upper panel; data from three experiments are summarized in the lower panel.

(E) Increased CHOP induction in MIN6Ei4ebp1^{-/-} cells treated with thapsigargin. Representative blots are shown in the upper panel; data from four experiments are summarized in the lower panel.

(F) Chop mRNA levels in MIN6WT and MIN6Ei4ebp1^{-/-} cells treated with thapsigargin.

(G) Greater Chop translation in MIN6Ei4ebp1^{-/-} cells treated with thapsigargin. MIN6WT and MIN6Ei4ebp1^{-/-} cells treated with vehicle (C) or thapsigargin (Tg) for 12 hr were labeled with [³⁵S]methionine/cysteine. Lysates were either directly subjected to SDS-PAGE or immunoprecipitated with anti-CHOP antibody. Representative autoradiograms are shown in the left panel; data from four experiments are summarized in the right panel.

Error bars represent SEM. *p < 0.05, **p < 0.01.

4E-BP1-Deficient β Cells Are More Vulnerable to ER Stress

A 4E-BP1-deficient β cell line, MIN6*Eif4ebp1*^{-/-}, was established by crossing *Eif4ebp1*^{-/-} mice (Tsukiyama-Kohara et al., 2001) with IT6 mice expressing SV40 large T antigen in β cells (Miyazaki et al., 1990). MIN6 cells with wild-type *Eif4ebp1* alleles, established in parallel, were designated MIN6WT cells. MIN6*Eif4ebp1*^{-/-} cells were more vulnerable to ER stress inducers than MIN6WT cells (Figure 3A). 4E-BP1 re-expression restored this diminished viability of MIN6*Eif4ebp1*^{-/-} cells to control levels (Figure S3A). The increased susceptibility to ER stress-induced cell death was accompanied by enhanced caspase-3 cleavage (Figure 3B), indicating that the reduced viability of MIN6*Eif4ebp1*^{-/-} cells was due at least in part to increased apoptosis. In addition, DNA fragmentation under ER stress was greater in *Eif4ebp1*^{-/-} islets than in wild-type islets (Figure S3B). These results suggest that 4E-BP1 induction contributes to β cell survival under ER stress.

We then examined the impact of 4E-BP1 deficiency on the integrity of the eIF4E translational initiation complex. Pull-down assays of eIF4E and its binding partners with a cap analog, 7-methyl-GTP, revealed that thapsigargin-induced 4E-BP1 expression resulted in marked increases in the amounts of hypophosphorylated 4E-BP1 α and β forms bound to eIF4E, displacing eIF4G from eIF4E in MIN6WT cells (Figure 3C, compare lane 5 with lane 6). The amount of eIF4G bound to eIF4E was reduced to 63% \pm 3% (n = 4, p < 0.05) of that in vehicle-treated MIN6WT cells. In contrast, levels of eIF4G bound to eIF4E were not decreased by thapsigargin in MIN6*Eif4ebp1*^{-/-} cells (Figure 3C, compare lane 7 with lane 8). Thus, eIF4E availability for translational initiation was greater in MIN6*Eif4ebp1*^{-/-} cells than in MIN6WT cells under ER stress. Measurement of the global translation rate revealed that recovery from translational suppression by thapsigargin was more rapid in 4E-BP1-deficient cells (Figure 3D).

Translation of newly synthesized mRNA molecules is reportedly much more dependent on eIF4E availability than that of preexisting mRNAs (Novoa and Carrasco, 1999). Expression of CHOP, a mediator of ER stress-induced apoptosis, was thus studied in MIN6*Eif4ebp1*^{-/-} cells since *Chop* mRNA is one of the transcripts most abundantly synthesized during ER stress (Pilot et al., 2007). *Eif4ebp1* deletion caused greater CHOP protein induction by thapsigargin in MIN6 cells (Figure 3E), with unaltered *Chop* mRNA accumulation (Figure 3F). Pulse-labeling experiments demonstrated enhanced CHOP translation (Figure 3G). Thus, CHOP expression during ER stress was augmented via increased translation in 4E-BP1 deficiency.

Eif4ebp1 Deletion Accelerates β Cell Loss in Mouse Diabetes Models

To examine the roles of 4E-BP1 under ER stress in vivo, *Eif4ebp1*^{-/-} mice on the 129S6 background were fed a high-fat diet (HFD), which is thought to produce ER stress in β cells through peripheral insulin resistance (Scheuner et al., 2005). *Eif4ebp1*^{-/-} mice developed glucose intolerance (Figures S4A and S4B), which was associated with blunted insulin secretion (Figure S4C) and reduced pancreatic insulin content (Figure S4D) as compared to HFD-fed wild-type mice. These data suggest that *Eif4ebp1*^{-/-} mice have a β cell defect. However, HFD-fed

Eif4ebp1^{-/-} mice gained more weight and were more insulin resistant than HFD-fed wild-type mice (Figures S4E and S4F). Therefore, the possibility remains that β cell failure in HFD-fed *Eif4ebp1*^{-/-} mice resulted from greater ER stress rather than from a defect in β cells lacking 4E-BP1.

We next crossed *Eif4ebp1*^{-/-} mice with two genetic models of diabetes in which β cells are under ER stress, *Ins2*^{WT/C96Y} and *Wfs1*^{-/-} mice on the 129S6 background. 4E-BP1 deficiency did not alter body weight (Figures S5A and S5B) or insulin sensitivity (Figures S5C and S5D) but worsened hyperglycemia in *Ins2*^{WT/C96Y} (Figure 4A) and *Wfs1*^{-/-} (Figure 4B) mice. In *Eif4ebp1*^{-/-} *Ins2*^{WT/C96Y} mice, pancreatic insulin content was less than half of that in *Ins2*^{WT/C96Y} mice at 5 weeks of age (Figure 4C), and the majority of islets in *Eif4ebp1*^{-/-} *Ins2*^{WT/C96Y} mice were smaller as compared to those in *Ins2*^{WT/C96Y} mice (Figure 4D). We also observed a 38% decrease in pancreatic insulin content in *Eif4ebp1*^{-/-} *Wfs1*^{-/-} mice as compared to *Wfs1*^{-/-} mice (Figure 4E). Importantly, the insulin-positive area was smaller in pancreatic sections from *Eif4ebp1*^{-/-} *Wfs1*^{-/-} mice than in pancreatic sections from *Wfs1*^{-/-} mice at 27–30 weeks of age (Figure 4F), indicating that ER stress-mediated β cell loss is exacerbated by 4E-BP1 deficiency in vivo.

Global protein synthesis was studied in these mouse islets. A tendency toward decreased protein synthesis was observed in both *Ins2*^{WT/C96Y} (Figure 4G, hatched bar; p = 0.074) and *Wfs1*^{-/-} islets (Figure 4H, hatched bar; p = 0.079) as compared to wild-type islets. *Eif4ebp1* deletion ablated this regulation and resulted in significantly increased protein synthesis in *Eif4ebp1*^{-/-} *Ins2*^{WT/C96Y} (p = 0.013) and *Eif4ebp1*^{-/-} *Wfs1*^{-/-} (p = 0.045) islets as compared to that in corresponding single mutants (compared hatched with filled bars in Figures 4G and 4H). These data suggest that accelerated β cell loss under ER stress is due to deregulated translational control.

DISCUSSION

Our results implicate 4E-BP1, identified as a component of the UPR, in β cell survival under ER stress. Important roles of 4E-BPs under various stress conditions have been recently demonstrated in yeast (Ibrahim et al., 2006) and *Drosophila* (Teleman et al., 2005; Tettweiler et al., 2005). These data suggest that translational suppression by 4E-BPs is an evolutionarily conserved strategy against stress conditions. Although we focused on β cells, ER stress-mediated induction of 4E-BP1 was also observed in the liver and kidneys, suggesting the general importance of the present findings.

Our results suggest that, in addition to translational regulation by eIF2 α phosphorylation due to PERK activation, another mode of translational control mediated by 4E-BP1 plays a role in the maintenance of β cell homeostasis under ER stress. Since translational suppression by eIF2 α phosphorylation is transient owing to feedback dephosphorylation by GADD34 (Novoa et al., 2001), prolonged translational suppression by 4E-BP1 might be needed in the later stages of the UPR. However, in contrast to PERK, 4E-BP1 deficiency alone does not cause diabetes in mice under normal conditions, suggesting that 4E-BP1 protein is not a key regulator but rather functions with other molecules to maintain β cell homeostasis under ER stress. The preferential role of 4E-BP1 in the later stages of the UPR might be puzzling since expression of

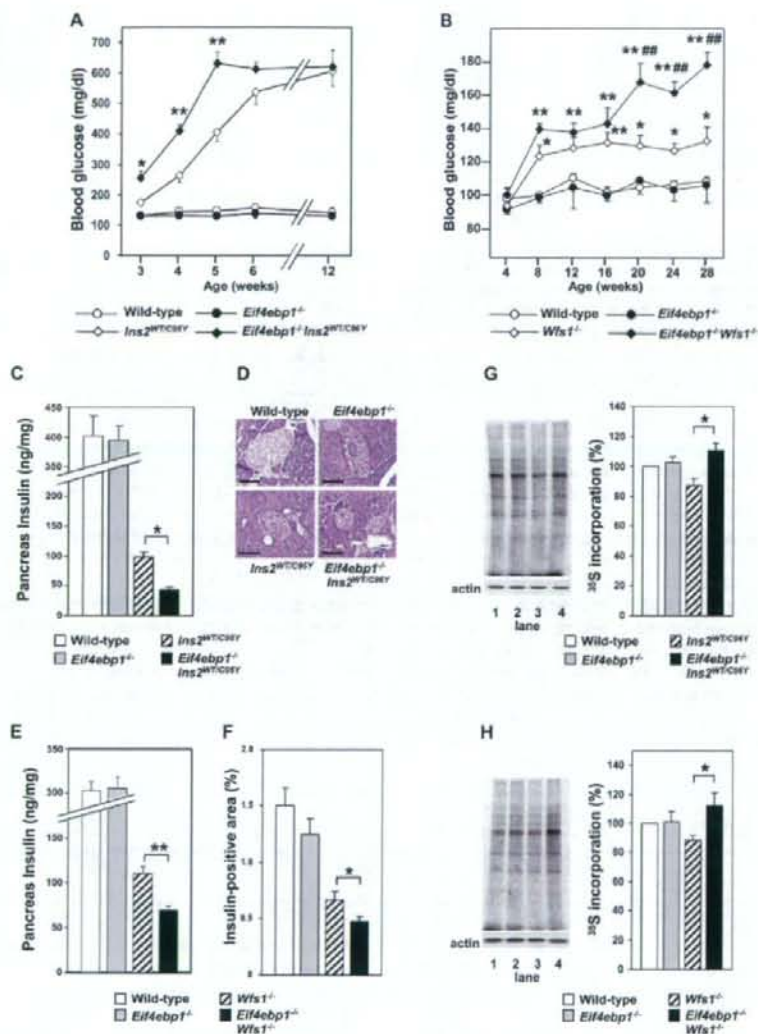


Figure 4. β Cell Loss Is Exacerbated by 4E-BP1 Deficiency in Mouse Diabetes Models

(A) Fed blood glucose levels of wild-type ($n = 6$), *Eif4ebp1*^{-/-} ($n = 5$), *Ins2*^{WT/CS8Y} ($n = 9$), and *Eif4ebp1*^{-/-}*Ins2*^{WT/CS8Y} ($n = 11$) mice. Data from three cohorts are combined. * $p < 0.05$, ** $p < 0.01$ versus wild-type mice; ## $p < 0.01$ versus *Ins2*^{WT/CS8Y} mice.

(B) Fed blood glucose levels of wild-type ($n = 12$), *Eif4ebp1*^{-/-} ($n = 8$), *Wfs1*^{-/-} ($n = 15$), and *Eif4ebp1*^{-/-}*Wfs1*^{-/-} ($n = 10$) mice. Data from three cohorts are combined. * $p < 0.05$, ** $p < 0.01$ versus wild-type mice; ## $p < 0.01$ versus *Wfs1*^{-/-} mice.

(C) Pancreatic insulin content of mice of the indicated genotypes at 5 weeks of age. $n = 3$ for each genotype. * $p < 0.05$.

(D) Hematoxylin and eosin staining of sections showing representative islets from mice of the indicated genotypes at 5 weeks of age. Scale bars = 50 μ m.

(E) Pancreatic insulin content of wild-type ($n = 8$), *Eif4ebp1*^{-/-} ($n = 4$), *Wfs1*^{-/-} ($n = 15$), and *Eif4ebp1*^{-/-}*Wfs1*^{-/-} ($n = 12$) mice at 27–30 weeks of age. ** $p < 0.01$.

(F) Insulin-positive area in pancreatic sections of wild-type ($n = 3$), *Eif4ebp1*^{-/-} ($n = 3$), *Wfs1*^{-/-} ($n = 4$), and *Eif4ebp1*^{-/-}*Wfs1*^{-/-} ($n = 5$) mice at 27–30 weeks of age. * $p < 0.05$.

(G) [³⁵S]methionine/cysteine incorporation in islets of the indicated genotypes at 5–6 weeks of age. Ten percent of the lysates were also probed with an anti-actin antibody. A representative autoradiogram is shown in the left panel. Lane 1, wild-type; lane 2, *Eif4ebp1*^{-/-}; lane 3, *Ins2*^{WT/CS8Y}; lane 4, *Eif4ebp1*^{-/-}*Ins2*^{WT/CS8Y}.

Data from four experiments are summarized in the right panel. * $p < 0.05$.

ATF4, the primary inducer of *Eif4ebp1* under ER stress, is activated by translational suppression by eIF2 α phosphorylation during the acute phase. We found that 4E-BP1 protein is stable with a half-life of approximately 20 hr (Figure S6). Thus, 4E-BP1 protein seems to continue to be expressed abundantly during the later stages of the UPR. This is consistent with the recent observation that several prosurvival proteins involved in the UPR are stable, while proapoptotic proteins are not (Rutkowski et al., 2006). We found that global protein synthesis was higher in 4E-BP1-deficient β cells than in wild-type cells under ER stress conditions. In particular, expression of CHOP was augmented in 4E-BP1 deficiency. Enhanced CHOP expression in 4E-BP1-deficient cells suggests that a reduction in eIF4E availability due to 4E-BP1 induction suppresses CHOP translation during ER stress in wild-type cells, possibly accounting for one of the mechanisms by which 4E-BP1 plays a role in adaptation to ER stress. Important roles of translational control via eIF4E availability have also been suggested in prolonged hypoxia (Koritzinsky et al., 2006). However, the signaling mechanisms for translational control are different: ER stress increases 4E-BP1 protein levels via ATF4 in β cells, while hypoxia enhances 4E-BP1 activity via dephosphorylation and also causes eIF4E nuclear localization in HeLa cells.

The present results also suggest that variations in genes regulating eIF4E availability and/or eIF4F formation may have an impact on susceptibility to diabetes. In this context, a recent report demonstrating that a gene encoding eIF4A2, a component of eIF4F, is possibly linked to type 2 diabetes in French families (Cheyssac et al., 2006) is of great interest. Furthermore, our findings raise the possibility that 4E-BP1 may be a potential target for diabetes mellitus treatment.

EXPERIMENTAL PROCEDURES

Animal Experiments

All animal experiments were approved by the Tohoku University Institutional Animal Care and Use Committee. *Wfs1*^{-/-} mice were backcrossed to a 129S6 (Taconic) background for six generations. *Ins2*^{WT/CreM} mice (Charles River Laboratories) were backcrossed to a 129S6 background for five generations. *Eif4ebp1*^{-/-} mice were maintained on a 129S6 background. Only male mice were used. For the in vivo studies shown in Figures 4A, 4C, and 4D, littermates from crosses of male *Ins2*^{WT/CreM} *Eif4ebp1*^{+/-} and female *Ins2*^{WT/WT} *Eif4ebp1*^{+/-} mice were used. For Figures 4B, 4E, and 4F, littermates from intercrosses of *Eif4ebp1*^{+/-} *Wfs1*^{+/+} mice and littermates from intercrosses of *Eif4ebp1*^{+/-} *Wfs1*^{-/-} mice were used. For isolated islet experiments (Figures 4G and 4H), age-matched nonlittermate mice were used. To induce ER stress in vivo, mice were given a 0.5 μ g/g body weight intraperitoneal injection of tunicamycin. After 96 hr, kidneys and livers were removed. Tissue sample processing, immunostaining of pancreatic sections, and determination of β cell area and pancreatic insulin content were performed as described previously (Ishihara et al., 2004).

Cell Culture and Cell Viability Assay

Pancreatic tumors in *Eif4ebp1*^{-/-}:SV40Tag mice on a mixed background were excised, yielding MIN6/*Eif4ebp1*^{-/-} cells, which were used at 5–10 passages in this study. MIN6 cells were cultured in DMEM supplemented with 15% FCS. *Atf4*^{-/-} MEFs were cultured in DMEM supplemented with a nonessential amino acid mixture and 10% FCS. Cells seeded in 24-well plates 2 days previously were treated with thapsigargin or tunicamycin and used for western blotting or cell viability assay. Cell viability was determined with a cell prolifer-

ation assay kit (Promega). Construction of adenoviruses and infection of MIN6 cells were performed as described previously (Ishihara et al., 2004).

Northern and Western Blotting and Cap-Binding Affinity Assay

Total RNA extracted using ISOGEN (Nippon Gene) was probed with ³²P-labeled cDNAs. Tissue homogenates and cell lysates were subjected to SDS-PAGE and probed with primary antibodies against 4E-BP1, 4E-BP2, eIF4E, eIF4G, cleaved caspase-3 (Cell Signaling), ATF4, CHOP (Santa Cruz), and actin (Sigma). Cell lysates were incubated with 7-methyl-GTP (³mGTP)-Sephacrose (Amersham) overnight at 4°C. The ³mGTP-Sephacrose was then pelleted and boiled. Experiments were performed at least three times. Band intensity was quantified using Scion Image software.

Metabolic Labeling

Due to the low islet yields from *Ins2*^{WT/CreM}, *Ins2*^{WT/CreM} *Eif4ebp1*^{-/-}, *Wfs1*^{-/-}, and *Eif4ebp1*^{-/-} *Wfs1*^{-/-} mice, islets with these genotypes were pooled from two or three mice. Fifty to eighty islets were cultured for 3 days in RPMI supplemented with 10% FCS. Islets washed with methionine/cysteine-free RPMI containing 10% dialyzed FCS were labeled with a protein labeling mix (PerkinElmer) (1.0 MBq/tube) for 15 min and then resolved in sample buffer (1.0 μ l/islet for wild-type and *Eif4ebp1*^{-/-} islets and 0.75 μ l/islet for other genotypes). The level of protein synthesis was quantified from autoradiograms. For measurement of Chop translation, 4 \times 10⁶ cells treated with thapsigargin for 12 hr were washed with methionine/cysteine-free DMEM containing 15% dialyzed FCS and labeled with [³⁵S]methionine/cysteine (20 MBq/bottle) for 2 hr. Cells were then resolved in lysis buffer (50 mM Tris [pH 7.5], 150 mM NaCl, 2 mM MgCl₂, 0.1% Triton X-100, and protease inhibitors [Roche]). Lysates were precleared with Protein A Sepharose Fast Flow (Amersham) and incubated with anti-CHOP antibody (R-20, Santa Cruz) overnight.

Firefly Luciferase Reporter Assay

Oligonucleotides containing ATF4 binding sites were annealed and subcloned into the pGL3-Promoter vector (BamHI-SalI, Promega). MIN6 cells were transfected with luciferase reporters using Lipofectamine (Invitrogen). Luciferase activity was assayed with a dual-luciferase system (Promega) using a luminometer (Berthold).

Chromatin Immunoprecipitation Assay

Proteins bound to DNA were crosslinked with 1% formaldehyde at 4°C for 20 min. After sonication, the protein-DNA complexes were immunoprecipitated using an anti-ATF4 antibody (C-20, Santa Cruz). After reversal of the crosslinks at 65°C for 6 hr, DNA was purified on a DNA purification column (QIAGEN). PCR was performed with the primers 5'-GATGAGGAGGAGGAGCTGAGT TG-3' and 5'-AGTTGTAAGAGGAGTGTGGGG-3'.

Statistical Analysis

Data are presented as means \pm SEM. Differences between groups were assessed by Student's t test. $p < 0.05$ was considered significant.

SUPPLEMENTAL DATA

Supplemental Data include six figures and Supplemental References and can be found with this article online at <http://www.celmetabolism.org/cgi/content/full/7/3/269/DC1/>.

ACKNOWLEDGMENTS

We thank J. Alam (Alton Ochsner Medical Foundation) and D. Ron (New York University) for their generous gifts of DN-ATF4 cDNA and *Atf4*^{-/-} MEFs, respectively. We are also grateful to K. Igarashi (Tohoku University) for advice on ChIP analysis and to Y. Nagura and K. Tanaka for their expert technical assistance. This work was supported by Grants-in-Aid for Scientific Research

(H) [³⁵S]methionine/cysteine labeling as in (G) in islets of the indicated genotypes at 6–8 weeks of age. Lane 1, wild-type; lane 2, *Eif4ebp1*^{-/-}; lane 3, *Wfs1*^{+/-}; lane 4, *Eif4ebp1*^{-/-} *Wfs1*^{-/-}. Data from three experiments are summarized in the right panel. * $p < 0.05$. Error bars represent SEM.

(19590300 to H.J. and 19209034 to Y.O.) from the Ministry of Education, Culture, Sports, Science and Technology of Japan.

Received: July 10, 2007

Revised: December 2, 2007

Accepted: January 30, 2008

Published: March 4, 2008

REFERENCES

- Butler, A.E., Janson, J., Bonner-Weir, S., Ritzel, R., Rizza, R.A., and Butler, P.C. (2003). β -cell deficit and increased beta-cell apoptosis in humans with type 2 diabetes. *Diabetes* 52, 102–110.
- Cheysac, C., Dina, C., Laprete, F., Vasseur-Delannoy, V., Dechaume, A., Lobbens, S., Balkau, B., Ruiz, J., Charpentier, G., Pattou, F., et al. (2006). EIF4A2 is a positional candidate gene at the 3q27 locus linked to type 2 diabetes in French families. *Diabetes* 55, 1171–1176.
- Clemens, M.J. (2001). Translational regulation in cell stress and apoptosis. Roles of the eIF4E binding proteins. *J. Cell. Mol. Med.* 5, 221–239.
- Delapine, M., Nicolino, M., Barrett, T., Golamaully, M., Lathrop, G.M., and Julier, C. (2000). EIF2AK3, encoding translation initiation factor 2-alpha kinase 3, is mutated in patients with Wolcott-Rallison syndrome. *Nat. Genet.* 25, 406–409.
- Harding, H.P., Novoa, I., Zhang, Y., Zeng, H., Wek, R., Schapira, M., and Ron, D. (2000). Regulated translation initiation controls stress-induced gene expression in mammalian cells. *Mol. Cell* 6, 1099–1108.
- Harding, H.P., Zeng, H., Zhang, Y., Jungries, R., Chung, P., Plesken, H., Sabatini, D.D., and Ron, D. (2001). Diabetes mellitus and exocrine pancreatic dysfunction in *per1* mice reveals a role for translational control in secretory cell survival. *Mol. Cell* 7, 1153–1163.
- Harding, H.P., Zhang, Y., Zeng, H., Novoa, I., Lu, P.D., Calfon, M., Sadri, N., Yun, C., Popko, B., Paules, R., et al. (2003). An integrated stress response regulates amino acid metabolism and resistance to oxidative stress. *Mol. Cell* 11, 619–633.
- He, C.H., Gong, P., Hu, B., Stewart, D., Choi, M.E., Choi, A.M., and Alam, J. (2001). Identification of activating transcription factor 4 (ATF4) as an Nrf2-interacting protein. Implication for heme oxygenase-1 gene regulation. *J. Biol. Chem.* 276, 20858–20865.
- Holcik, M., and Sonenberg, N. (2005). Translational control in stress and apoptosis. *Nat. Rev. Mol. Cell Biol.* 6, 318–327.
- Ibrahim, S., Holmes, L.E., and Asha, M.P. (2006). Regulation of translation initiation by the yeast eIF4E binding proteins is required for the pseudohyphal response. *Yeast* 23, 1075–1088.
- Inoue, H., Tanizawa, Y., Wasson, J., Behn, P., Kalidas, K., Bernal-Mizrachi, E., Mueckler, M., Marshall, H., Donis-Keller, H., Crock, P., et al. (1998). A gene encoding a transmembrane protein is mutated in patients with diabetes mellitus and optic atrophy (Wolfram syndrome). *Nat. Genet.* 20, 143–148.
- Ishihara, H., Takeda, S., Tamura, A., Takahashi, R., Yamaguchi, S., Takel, D., Yamada, T., Inoue, H., Soga, H., Katagiri, H., et al. (2004). Disruption of the *WFS1* gene in mice causes progressive beta-cell loss and impaired stimulus-secretion coupling in insulin secretion. *Hum. Mol. Genet.* 13, 1159–1170.
- Koritzinsky, M., Magagnoli, M.G., van den Beucken, T., Seigneure, R., Savelkoul, K., Dostie, J., Puyronnet, S., Kaufman, R.J., Weppler, S.A., Voncken, J.W., et al. (2006). Gene expression during acute and prolonged hypoxia is regulated by distinct mechanisms of translational control. *EMBO J.* 25, 1114–1125.
- Laybutt, D.R., Preston, A.M., Akerfeldt, M.C., Kench, J.G., Busch, A.K., Biankin, A.V., and Biden, T.J. (2007). Endoplasmic reticulum stress contributes to beta cell apoptosis in type 2 diabetes. *Diabetologia* 50, 752–763.
- Miyazaki, J., Araki, K., Yamato, E., Ikegami, H., Asano, T., Shibasaki, Y., Oka, Y., and Yamamura, K. (1990). Establishment of a pancreatic beta cell line that retains glucose-inducible insulin secretion: special reference to expression of glucose transporter isoforms. *Endocrinology* 127, 126–132.
- Novoa, I., and Carrasco, L. (1999). Cleavage of eukaryotic translation initiation factor 4G by exogenously added hybrid proteins containing poliovirus 2Apro in HeLa cells: effects on gene expression. *Mol. Cell Biol.* 19, 2445–2454.
- Novoa, I., Zeng, H., Harding, H.P., and Ron, D. (2001). Feedback inhibition of the unfolded protein response by GADD34-mediated dephosphorylation of eIF2 α . *J. Cell Biol.* 153, 1011–1022.
- Pirot, P., Naamane, N., Libert, F., Magnusson, N.E., Ortoft, T.F., Cardozo, A.K., and Eizirik, D.L. (2007). Global profiling of genes modified by endoplasmic reticulum stress in pancreatic beta cells reveals the early degradation of insulin mRNAs. *Diabetologia* 50, 1006–1014.
- Riggs, A.C., Bernal-Mizrachi, E., Ohsugi, M., Wasson, J., Fatrai, S., Welling, C., Murray, J., Schmidt, R.E., Herrera, P.L., and Pernutt, M.A. (2005). Mice conditionally lacking the *Wolfman* gene in pancreatic islet beta cells exhibit diabetes as a result of enhanced endoplasmic reticulum stress and apoptosis. *Diabetologia* 48, 2313–2321.
- Rutkowski, D.T., Arnold, S.M., Miller, C.N., Wu, J., Li, J., Gunnison, K.M., Mori, K., Sadighi Akha, A.A., Raden, D., and Kaufman, R.J. (2006). Adaptation to ER stress is mediated by differential stabilities of pro-survival and pro-apoptotic mRNAs and proteins. *PLoS Biol.* 4, e374.
- Scheuner, D., Mierde, D.V., Song, B., Flamez, D., Creemers, J.W., Tsukamoto, K., Ribick, M., Schult, F.C., and Kaufman, R.J. (2005). Control of mRNA translation preserves endoplasmic reticulum function in β cells and maintains glucose homeostasis. *Nat. Med.* 11, 757–764.
- Schroder, M., and Kaufman, R.J. (2005). The mammalian unfolded protein response. *Annu. Rev. Biochem.* 74, 739–789.
- Strom, T.M., Hortnagel, K., Hofmann, S., Gekeler, F., Scharfe, C., Rabi, W., Gerbitz, K.D., and Meltinger, T. (1998). Diabetes insipidus, diabetes mellitus, optic atrophy and deafness (DIDMOAD) caused by mutations in a novel gene (*wolframin*) coding for a predicted transmembrane protein. *Hum. Mol. Genet.* 7, 2021–2028.
- Teleman, A.A., Chen, Y.W., and Cohen, S.M. (2005). 4E-BP functions as a metabolic brake used under stress conditions but not during normal growth. *Genes Dev.* 19, 1844–1848.
- Tettweiler, G., Miron, M., Jenkins, M., Sonenberg, N., and Lasko, P.F. (2005). Starvation and oxidative stress resistance in *Drosophila* are mediated through the eIF4E-binding protein, d4E-BP. *Genes Dev.* 19, 1840–1843.
- Tsukiyama-Kohara, K., Poulin, F., Kohara, M., DeMaria, C.T., Cheng, A., Wu, Z., Gingras, A.C., Katsumi, A., Eicheby, M., Spiegelman, B.M., et al. (2001). Adipose tissue reduction in mice lacking the translational inhibitor 4E-BP1. *Nat. Med.* 7, 1128–1132.
- Wang, J., Takeuchi, T., Tanaka, S., Kubo, S.K., Kayo, T., Lu, D., Takata, K., Koizumi, A., and Izumi, T. (1999). A mutation in the insulin 2 gene induces diabetes with severe pancreatic β -cell dysfunction in the Mody mouse. *J. Clin. Invest.* 103, 27–37.
- Zhang, P., McGrath, B., Li, S., Frank, A., Zambito, F., Reinert, J., Gannon, M., Ma, K., McNaughton, K., and Cavener, D.R. (2002). The PERK eukaryotic initiation factor 2 α kinase is required for the development of the skeletal system, postnatal growth, and the function and viability of the pancreas. *Mol. Cell Biol.* 22, 3864–3874.

Supplemental Data

Short Article

**ATF4-Mediated Induction of 4E-BP1
Contributes to Pancreatic β Cell Survival
under Endoplasmic Reticulum Stress**

Suguru Yamaguchi, Hisamitsu Ishihara, Takahiro Yamada, Akira Tamura, Masahiro Usui, Ryu Tominaga, Yuichiro Munakata, Chihiro Satake, Hideki Katagiri, Fumi Tashiro, Hiroyuki Aburatani, Kyoko Tsukiyama-Kohara, Jun-ichi Miyazaki, Nahum Sonenberg, and Yoshitomo Oka

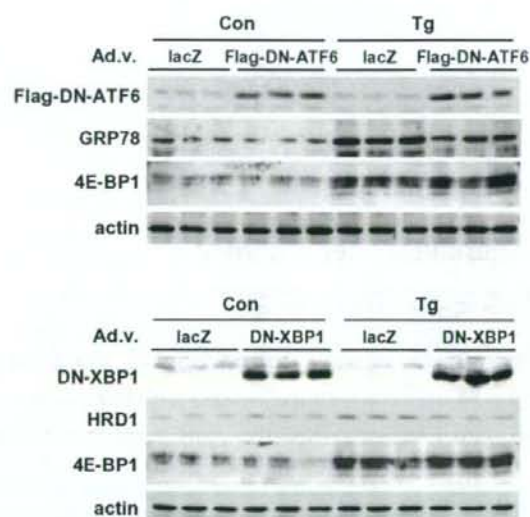


Figure S1. Effects of DN-ATF or DN-XBP1 Expression on 4E-BP1 Induction

Upper panel: no suppression of thapsigargin-triggered 4E-BP1 induction with expression of the Flag-tagged dominant-negative (DN) ATF6 (Flag-DN-ATF6: ATF6(171-373) lacking the activation domain (Yoshida et al., 2000)). MIN6 cells infected with an adenovirus expressing either lacZ or the Flag-DN-ATF6 were treated with vehicle (0.05% DMSO) control (Con) or thapsigargin (Tg, 0.5 μ M) for 12 hr. Cell lysates were analyzed for expressions of Flag-DN-ATF6, GRP78 (ATF6-target), 4E-BP1 and actin (loading control).

Lower panel: no suppression of Tg-triggered 4E-BP1 induction with expression of the DN-XBP1 (XBP1(1-188) lacking the activation domain (Lee et al., 2003)). MIN6 cells infected with an adenovirus expressing either lacZ or the DN-XBP1 were treated with vehicle control (Con) or Tg for 12 hr. Cell lysates were analyzed for expressions of DN-XBP1, HRD1 (XBP1-target), 4E-BP1 and actin (loading control).

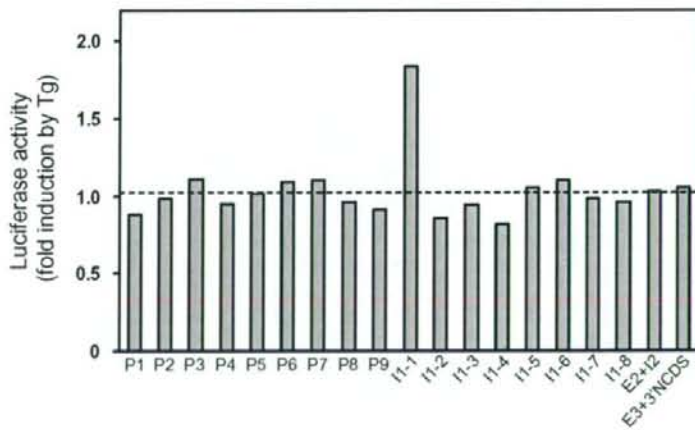
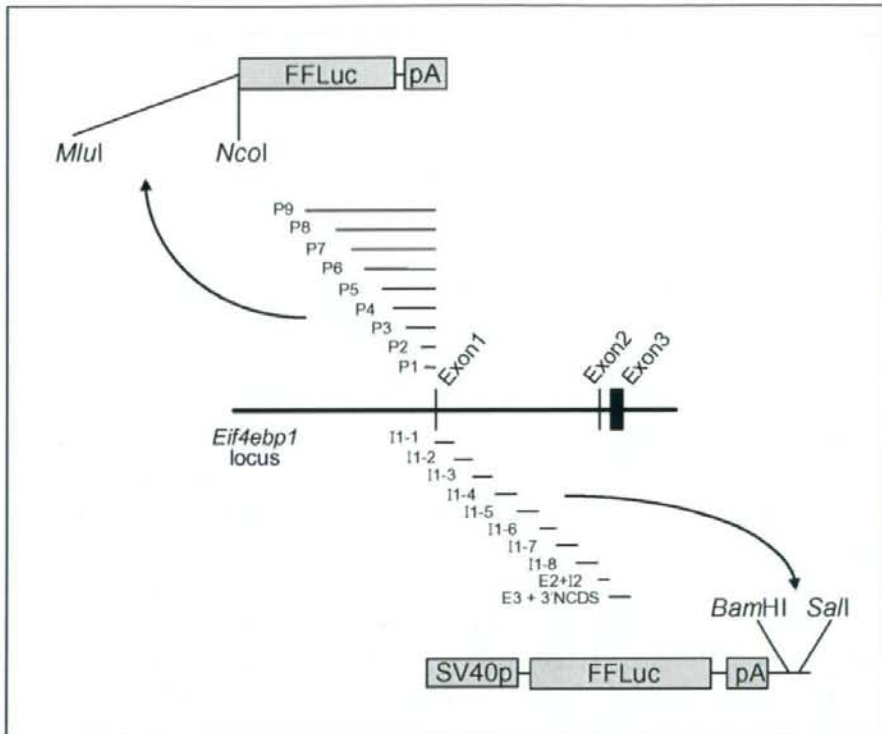


Figure S2. Search for Mouse *Eif4ebp1* Gene Segments Conferring Tg Responsiveness to Luciferase Reporter Constructs

Upper panel: reporter constructs used for luciferase activity measurements are presented. PCR-amplified *Eif4ebp1* promoter segments were cloned into the pGL3-basic construct (Promega). P1, -1 to -260 (A in the initial ATG codon is determined as +1); P2, -1 to -1,129; P3, -1 to -2,216; P4, -1 to -3,182; P5, -1 to -4,027; P6, -1 to -4,791; P7, -1 to -6,537; P8, -1 to -7,978; P9, -1 to -9,968. PCR-amplified *Eif4ebp1* segments spanning from exon 1 to the 3' non-coding sequence (3'NCDS) were cloned into the pGL3-promoter construct (Promega). I1-1, +1 to 1,821; I1-2, 1,821 to 3,409; I1-3, 3,409 to 5,198; I1-4, 5,198 to 6,957; I1-5, 6,957 to 8,752; I1-6, 8,752 to 9,977; I1-7, 9,977 to 11,804; I1-8, 11,804 to 12,949; E2+I2, 12,921 to 14,703; E3+3'NCDS, 14,704 to 16,260.

Lower panel: thapsigargin (Tg)-induced firefly luciferase activity in MIN6 cells transfected with reporter constructs shown in the upper panel. Firefly luciferase activity was normalized to Renilla luciferase activity and ratios of normalized activities in the presence to those in the absence of Tg are presented. Each experiment was performed employing 1 or 2 constructs and all data are presented together in one panel. Values are the means of 1 to 3 experiments, each performed in triplicate. Experiments were always conducted with a negative control construct (pGL3-promoter: a *SV40* promoter construct with no insertion between the *Bam*HI and *Sal*I sites) and a positive control construct (pGL3-basic with the *Chop* promoter). Fold inductions of the negative and positive controls were 1.03 ± 0.09 and 3.04 ± 0.11 -fold ($n = 25$), respectively. Data obtained with the negative control are shown as a dashed line.

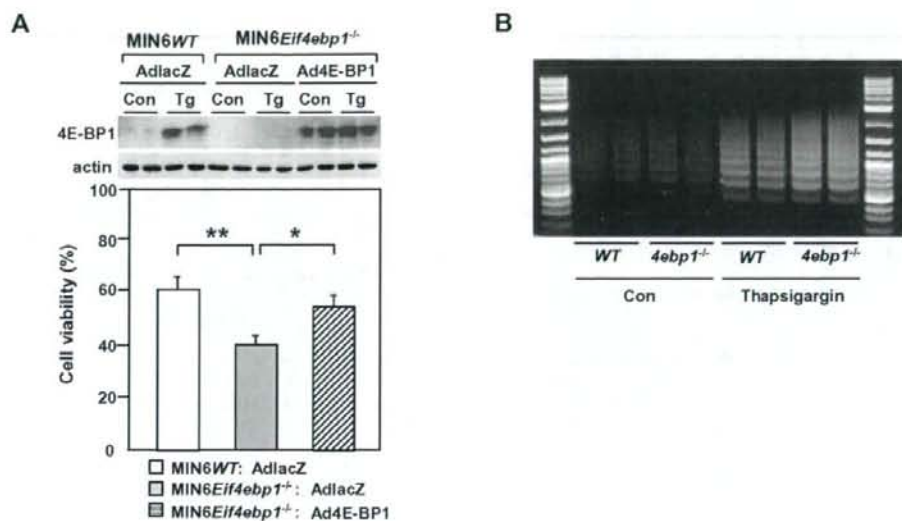


Figure S3. Higher Sensitivity of 4E-BP1-Deficient MIN6 Cells and Islets to ER Stress

(A) Reduced viability of MIN6^{Eif4ebp1^{-/-}} cells treated with 0.5 μ M thapsigargin (Tg) was restored by re-expression of 4E-BP1. Data from MIN6^{WT} cells treated with vehicle (0.05% DMSO) were taken as 100%. Error bars show SEM. n = 4; *p < 0.05, **p < 0.01.

Adenovirus-mediated re-expression of 4E-BP1 is shown in the upper panel. Con, vehicle-treated cells.

(B) Increased apoptotic DNA ladder formation in isolated islets from *Eif4ebp1^{-/-}* mice. Islets isolated from mice of each genotype at 12 weeks of age were incubated in RPMI medium for 3 days and DNA fragmentation was analyzed by ligation-mediated PCR as described previously (Ishihara et al., 2004).

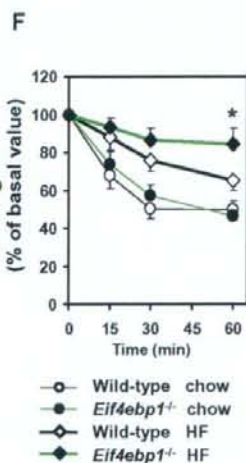
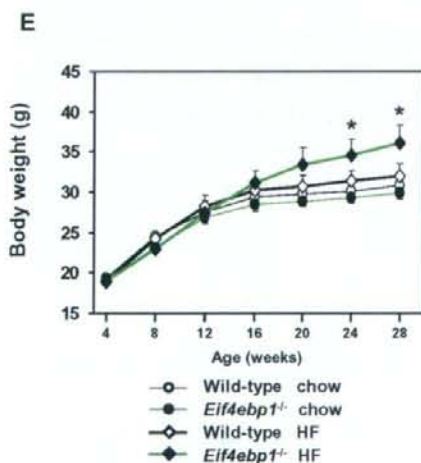
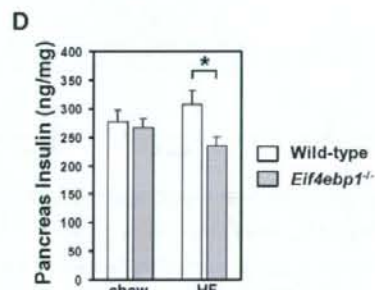
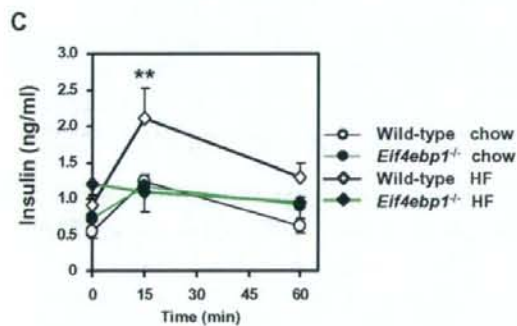
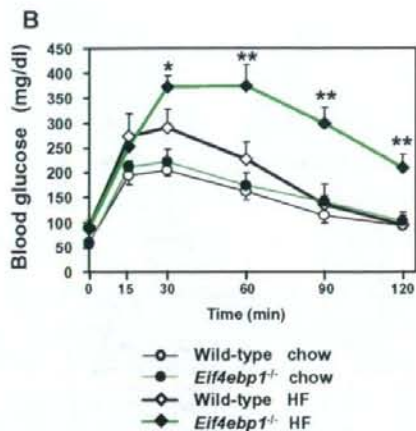
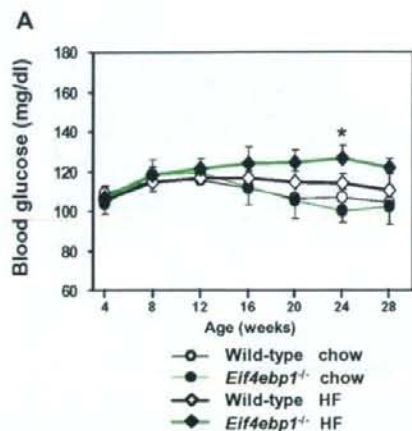


Figure S4. Body Weight and Glucose Homeostasis in Wild-Type and *Eif4ebp1*^{-/-} Mice Fed Standard Chow or a High-Fat Diet

(A) Fed blood glucose levels of wild-type and *Eif4ebp1*^{-/-} mice on standard chow or a high-fat diet (HFD; Research Diets D12451).

(B) Blood glucose levels during intraperitoneal glucose tolerance tests (2 g glucose per kg of body weight) in wild-type and *Eif4ebp1*^{-/-} mice fed chow or a HFD at 24 weeks of age.

(C) Plasma insulin levels during intraperitoneal glucose tolerance tests (2 g glucose per kg of body weight) in wild-type and *Eif4ebp1*^{-/-} mice fed chow or a HFD at 26 weeks of age.

(D) Pancreatic insulin contents of wild-type and *Eif4ebp1*^{-/-} mice fed chow or a HFD at 28 weeks of age.

(E) Growth curves of wild-type and *Eif4ebp1*^{-/-} mice fed chow or a HFD.

(F) Insulin tolerance tests in wild-type and *Eif4ebp1*^{-/-} mice fed chow or a HFD at 25 weeks of age. After a 6 hr fast, mice were given an intraperitoneal injection of insulin (0.75 μ U/g body weight). Blood glucose levels at time zero were 69 ± 5 (chow-fed wild-type), 84 ± 11 (chow-fed *Eif4ebp1*^{-/-}), 79 ± 5 (HFD-fed wild-type) and 107 ± 6 mg/dl (HFD-fed *Eif4ebp1*^{-/-}).

* $p < 0.05$ and ** $p < 0.01$, between HFD-fed *Eif4ebp1*^{-/-} and HFD-fed wild-type mice. $n = 4-6$.

Error bars show SEM.

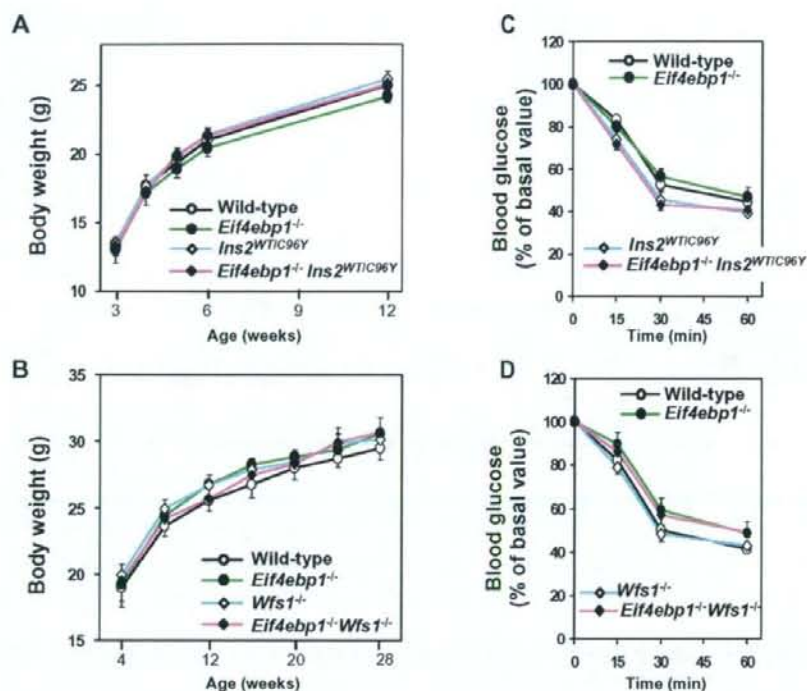


Figure S5. Characterization of 4E-BP1-Deficient *Ins2*^{WT/C96Y} and *Wfs1*^{-/-} Mice

(A) Growth curves of wild-type, *Eif4ebp1*^{-/-}, *Ins2*^{WT/C96Y} and *Eif4ebp1*^{-/-} *Ins2*^{WT/C96Y} mice. n = 5-11.

(B) Growth curves of wild-type, *Eif4ebp1*^{-/-}, *Wfs1*^{-/-} and *Eif4ebp1*^{-/-} *Wfs1*^{-/-} mice. n = 8-15.

(C) Intraperitoneal insulin tolerance tests in wild-type, *Eif4ebp1*^{-/-}, *Ins2*^{WT/C96Y} and *Eif4ebp1*^{-/-} *Ins2*^{WT/C96Y} mice at 5 weeks of age. After a 6 hr fast, mice were given an intraperitoneal injection of insulin (0.75 μ U/g body weight). Blood glucose levels at time zero were 77 \pm 6 (wild-type), 72 \pm 5 (*Eif4ebp1*^{-/-}), 216 \pm 19 (*Ins2*^{WT/C96Y}) and 271 \pm 23 mg/dl (*Eif4ebp1*^{-/-} *Ins2*^{WT/C96Y}). n = 5-8. Insulin sensitivities did not differ among the four groups.

(D) Insulin tolerance tests in wild-type, *Eif4ebp1*^{-/-}, *Wfs1*^{-/-} and *Eif4ebp1*^{-/-} *Wfs1*^{-/-} mice at 24 weeks of age. After a 6 hr fast (time zero), blood glucose was reduced to similar levels in all four groups; blood glucose levels at time zero were 79 \pm 6 (wild-type), 73 \pm 5 (*Eif4ebp1*^{-/-}), 80 \pm 7 (*Wfs1*^{-/-}) and 77 \pm 9 mg/dl (*Eif4ebp1*^{-/-} *Wfs1*^{-/-}). n = 7-9. Insulin sensitivities did not differ among the four groups (p > 0.094).

Error bars show SEM.